Published in Borneo Journal of Resource Science and Technology (2025), 15(1): 130-145
DOI: https:doi.org/10.33736/bjrst.7237.2025

SUPPLEMENTARY MATERIALS

Recognition of Sesquiterpenoids and Piperidine Alkamides as Two Discerning Metabolite Classes in the Fruits of *Piper nigrum* 'Semongok Aman'

MUHAMAD FARIS OSMAN*[1], SITI MUNIRAH MOHD FAUDZI [2,3], KHOZIRAH SHAARI[2], SHAHRUL RAZID SARBINI[4] & SHAMSUL KHAMIS[5,6]

[1]Pharmacognosy Research Group, Department of Pharmaceutical Chemistry, Kulliyyah of Pharmacy, International Islamic University Malaysia, Kuantan 25200, Pahang, Malaysia; [2]Natural Medicines and Products Research Laboratory, Institute of Bioscience, Universiti Putra Malaysia, 43400 UPM Serdang, Selangor, Malaysia; [3]Department of Chemistry, Faculty of Science, Universiti Putra Malaysia, 43400 UPM, Serdang. Selangor, Malaysia; [4]Department of Crop Science, Faculty of Agricultural and Forestry Sciences, Universiti Putra Malaysia, Bintulu 97008, Sarawak, Malaysia; [5]Department of Biological Sciences and Biotechnology, Faculty of Science and Technology, Universiti Kebangsaan Malaysia, UKM, Bangi 43600, Selangor, Malaysia; [6]Fraser's Hill Research Center, Natural and Physical Laboratory Management Center (ALAF-UKM) Research Complex, Universiti Kebangsaan Malaysia, UKM, Bangi 43600, Selangor, Malaysia
*Corresponding author: farisosman@iium.edu.my

Figure S1. *Piper nigrum* vines growing on dead *belian* (*Eusideroxylon zwageri* Teijsm. & Binn.) wooden poles as support at the pepper farm in Sebauh, Bintulu, Sarawak, Malaysia (left) and coordinates of the farm location (right). A more detailed view of the location is available online at http://bit.ly/40qAXt5

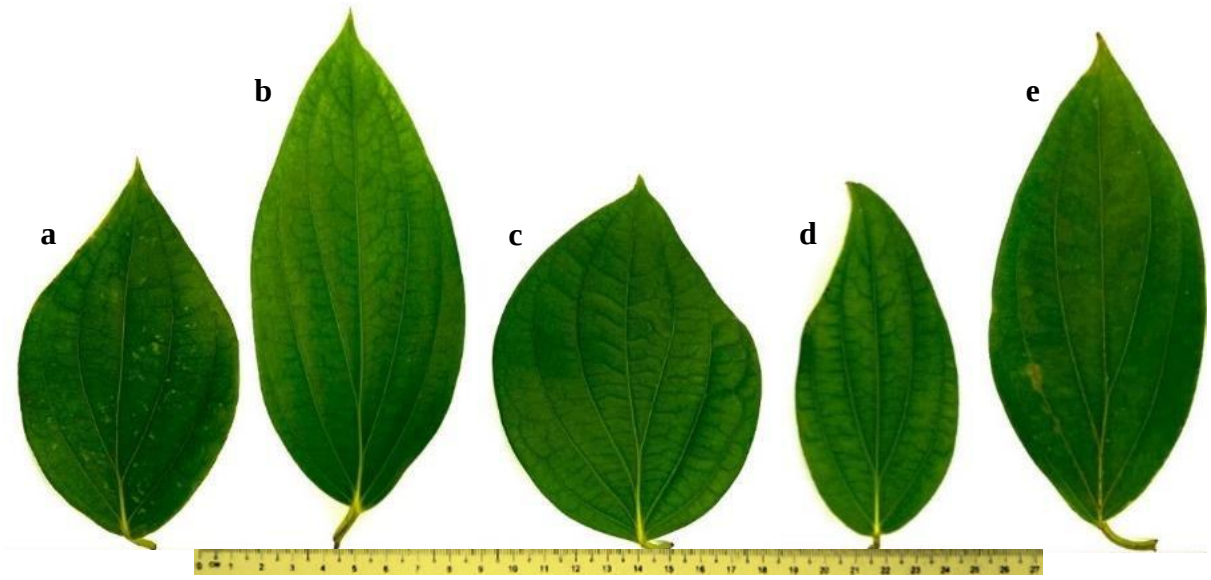

Figure S2. Leaves of the selected *Piper nigrum* cultivars: (**a**) 'Kuching', (**b**) 'Semongok Emas', (**c**) 'Semongok Aman', (**d**) 'India', and (**e**) 'Yong Petai'. The scale is in centimetres (cm)

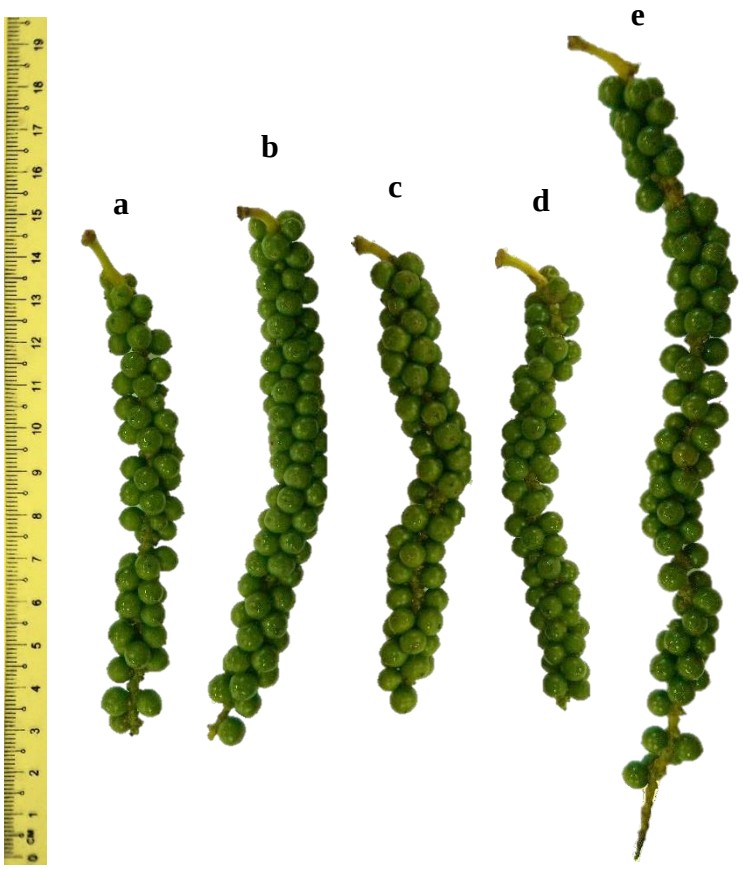

Figure S3. Fruit spikes of the selected *Piper nigrum* cultivars: (**a**) 'Kuching', (**b**) 'Semongok Emas', (**c**) 'Semongok Aman', (**d**) 'India', and (**e**) 'Yong Petai'. The scale is in centimetres (cm)

Figure S4. One-hour drying of cleaned *Piper nigrum* 'Semongok Aman' (A1–A8), 'Semongok Emas' (B1–B8), 'Kuching' (C1–C4), 'India' (D1–D8), and 'Yong Petai' (E1–E8) fruit spikes on unbleached parchment paper sheets in a laboratory at UPM Bintulu

Figure S4. (continued)

Figure S5. Three *Piper nigrum* fruit spikes bundled with a metal wire. A bundle of three fruit spikes represented a biological replicate

Figure S6. Lyophilised *Piper nigrum* fruit spikes (left) and a magnified view of two greem fruits of acceptable quality (right) detached from the fruit spikes. As several fruits were oxidised during the transportation from UPM Bintulu to UPM Serdang, only 30 fruits of uniform size that remained green were selected for further analysis from the bundled three fruit spikes

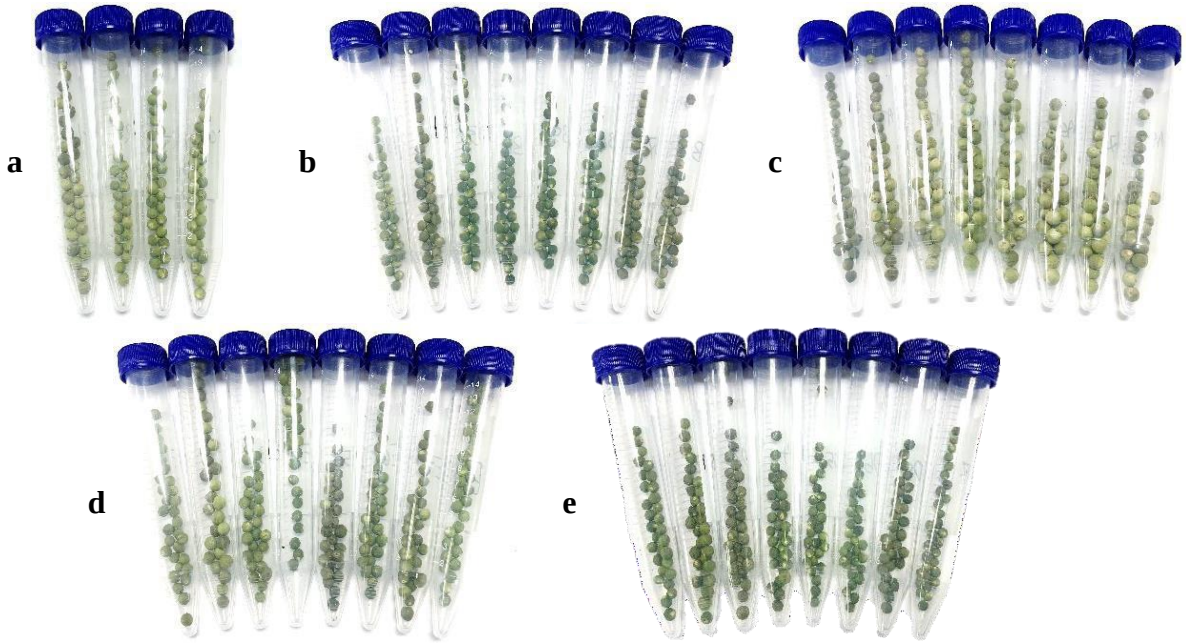

Figure S7. Selected lyophilised fruits of *Piper nigrum* cultivars: (**a**) 'Kuching' (*n* = 4), (**b**) 'Semongok Emas' (*n* = 8), (**c**) 'Semongok Aman' (*n* = 8), (**d**) 'India' (*n* = 8), and (**e**) 'Yong Petai' (*n* = 8)

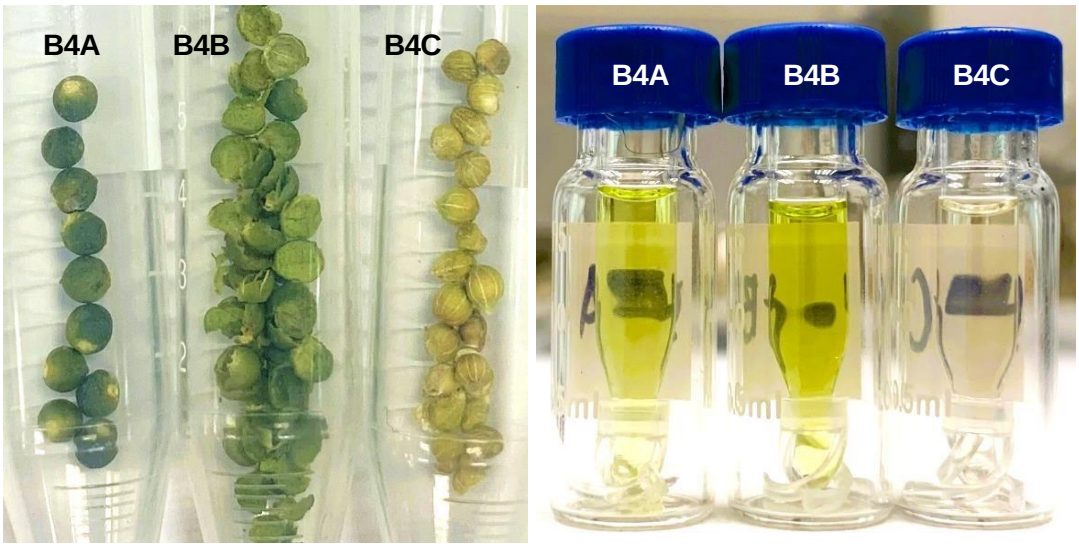

Figure S8. Lyophilised *Piper nigrum* fruit samples (left) and the respective *n*-hexane extracts (right). B4A: 10 whole fruits, B4B: exocarp and mesocarp of 20 fruits, and B4C: endocarp and seeds of 20 fruits of sample B4

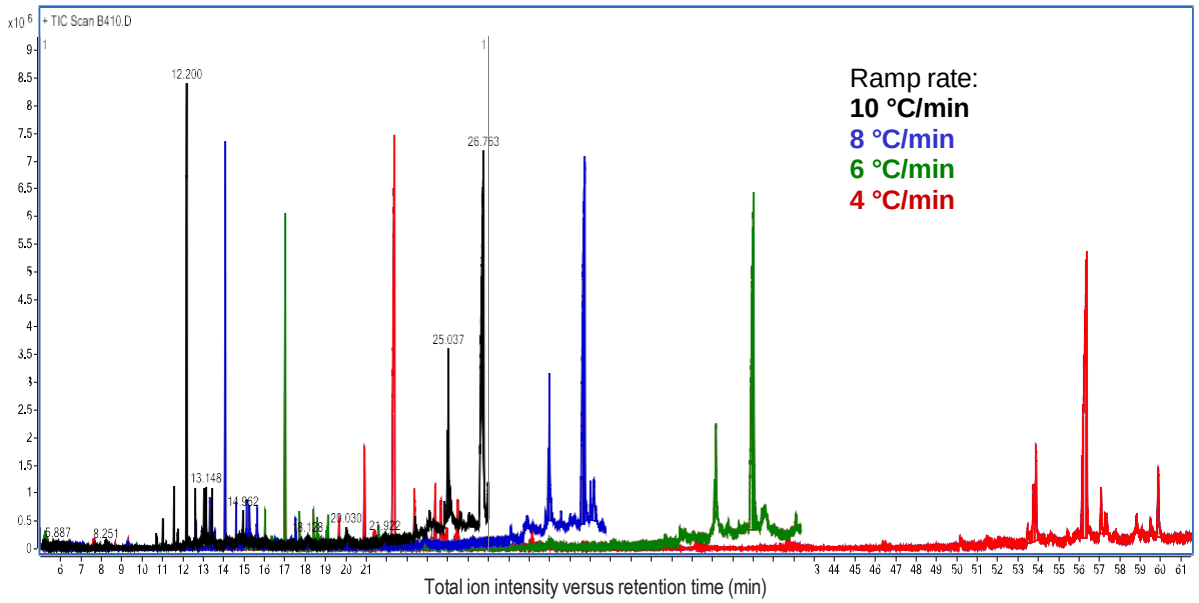

Figure S9. Overlaid total ion current (TIC) GC-MS chromatograms of sample B4A with varying ramp rates of oven temperature. In the preliminary study, the run time for GC-MS analysis of an *n*-hexane extract of *Piper nigrum* fruit was 110.0 min at a ramp rate of 2 °C/min. Therefore, it was necessary for GC-MS metabolomics to reduce the run time per sample without compromising data quality. The data quality of GC-MS, as indicated by the average similarity index of the matched spectral libraries, decreased with increasing ramp rate. Of the four GC oven temperature ramp rates tested, 4 °C/min was selected for GC-MS metabolomics because the average similarity index was highest using this ramp rate (80, acceptable range: 80−99) and the run time per sample could be reduced to 61.5 minutes

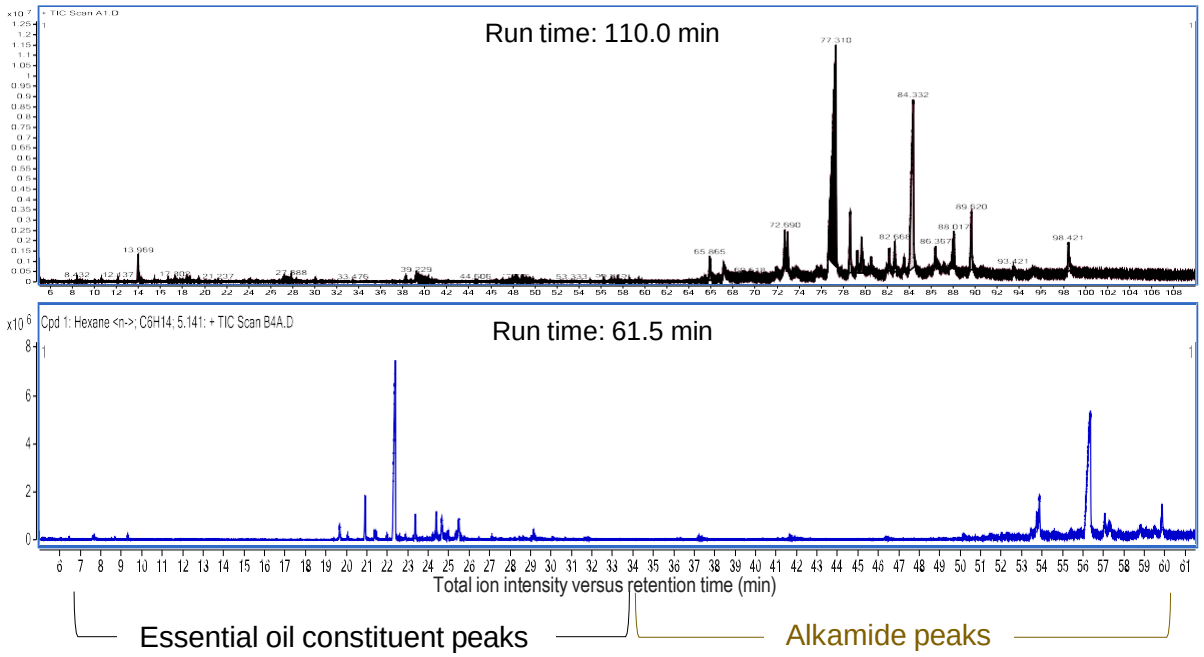

Figure S10. TIC GC-MS chromatograms of *n*-hexane extracts of *Piper nigrum* fruit in the preliminary study (top) and B4A (bottom). The fruit sample in the preliminary study was brown, while the B4A sample was green. The sample in the upper chromatogram was ground before it was lyophilised, while sample B4A was lyophilised before it was ground. The upper chromatogram shows that more volatile metabolites, i.e., the essential oil components, were lost when the sample was ground before lyophilisation. In contrast, the essential oil constituents were retained when the sample was lyophilised prior to grinding. Compared to the lower chromatogram, a greater number of alkamide peaks were observed in the upper chromatogram. This may be attributed to the lower rate of increase in GC oven temperature and possibly the detection of oxidised metabolites in the fruit extract. To reduce the size of the data files, the m/z range for the analysis of sample B4A was changed from 50−700 to 30−350

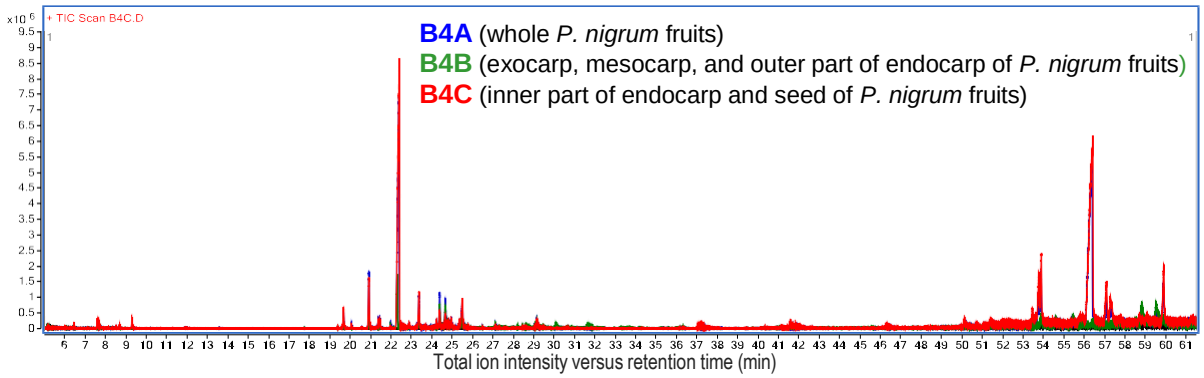

Figure S11. Overlaid TIC GC-MS chromatograms of *n*-hexane extracts of samples B4A, B4B, and B4C. Compared with the skin (B4B), a much higher abundance of *Piper nigrum* fruit metabolites were detected in the inner part of the endocarp and in the seed (B4C). This finding suggest that the metabolite profile of the endocarp and seed is more representative of the fruit than that of the skin. However, the removal of the fruit's skin is a laborious task and consequently could lead to oxidation of the seed. Therefore, the whole fruit was selected as the sample for GC-MS and ^{1}H-NMR metabolomics of *P. nigrum* fruits

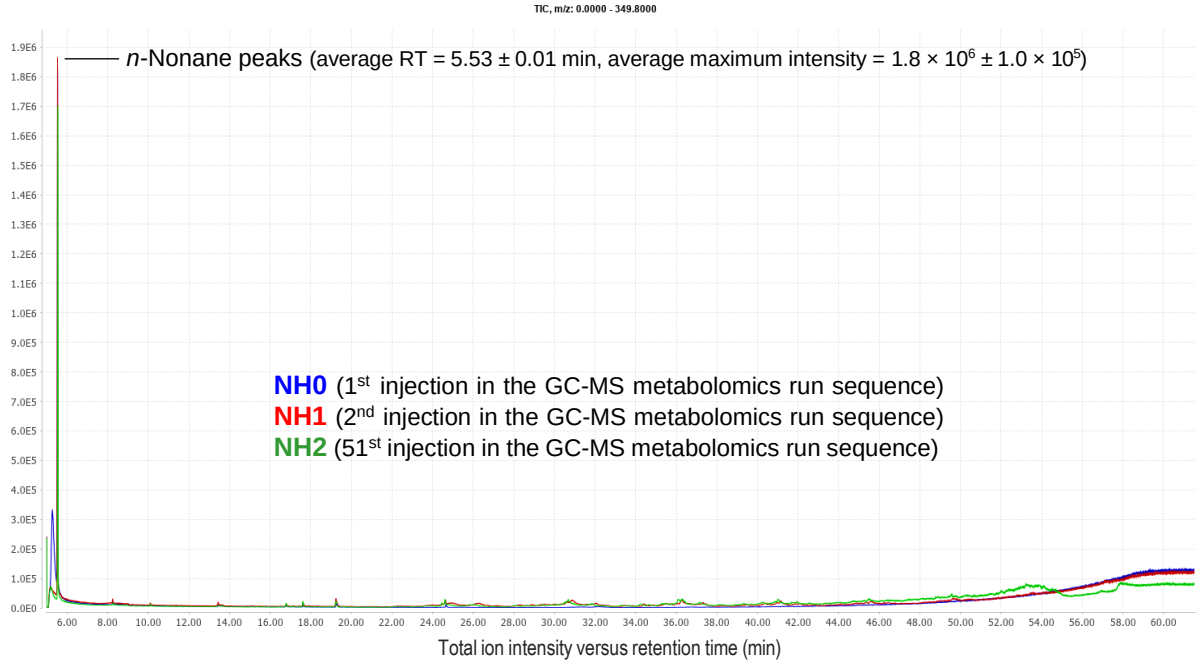

Figure S12. Overlaid TIC GC-MS chromatograms of extraction solvent blanks NH0, NH1, and NH2. The maximum intensities of the baseline and impurity peaks (i.e., intensity range: 6.0×10^2–1.4×10^5) were considered low, indicating that all blanks did not undergo significant changes throughout the run sequence. The variations in retention time shift and maximum intensity of the *n*-nonane (internal standard) peaks were also low (RSD 0.18 and 5.56%, respectively), indicating that normalisation of the preprocessed GC-MS data based on the peak intensities of the internal standard is a reasonable method for the present research

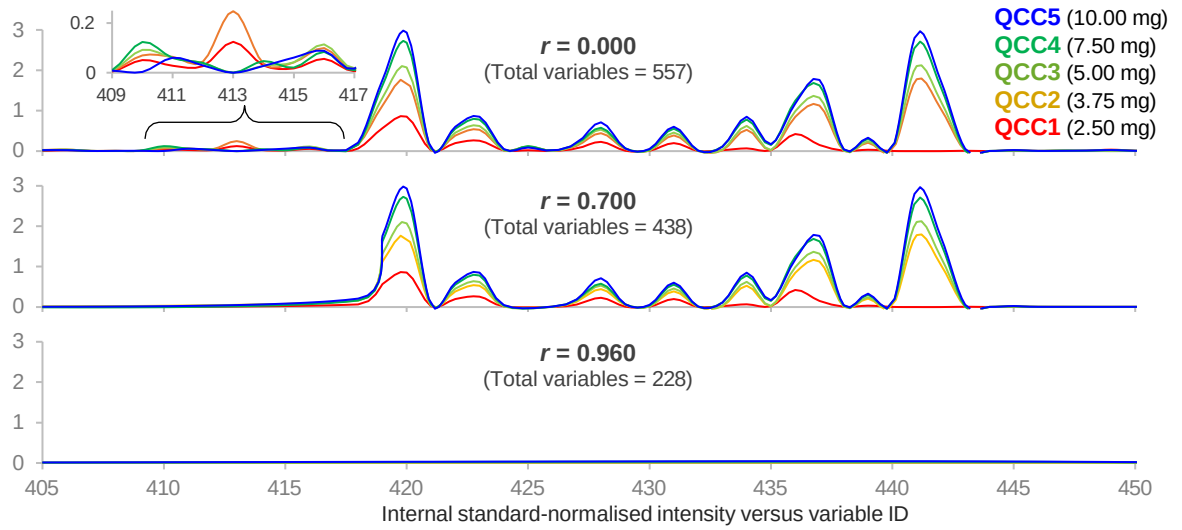

Figure S13. Example of the effect of different bivariate Pearson's correlation coefficients (r) in the QC calibration curve filtering on GC-MS chromatographic features. Note the noise (i.e., variable ID 409−417) among the preprocessed features (top). A moderate value of r allowed the desired retention of important features and reasonable removal of noise (middle), while a high value of r resulted in significant removal of the important features and noise (bottom)

Figure S14. Occurrence of black precipitates at the bottom of NMR tubes containing aqueous methanolic extracts of *Piper nigrum* fruits. The precipitates were absent during the extracts preparation and appeared only at the time of NMR spectra acquisition

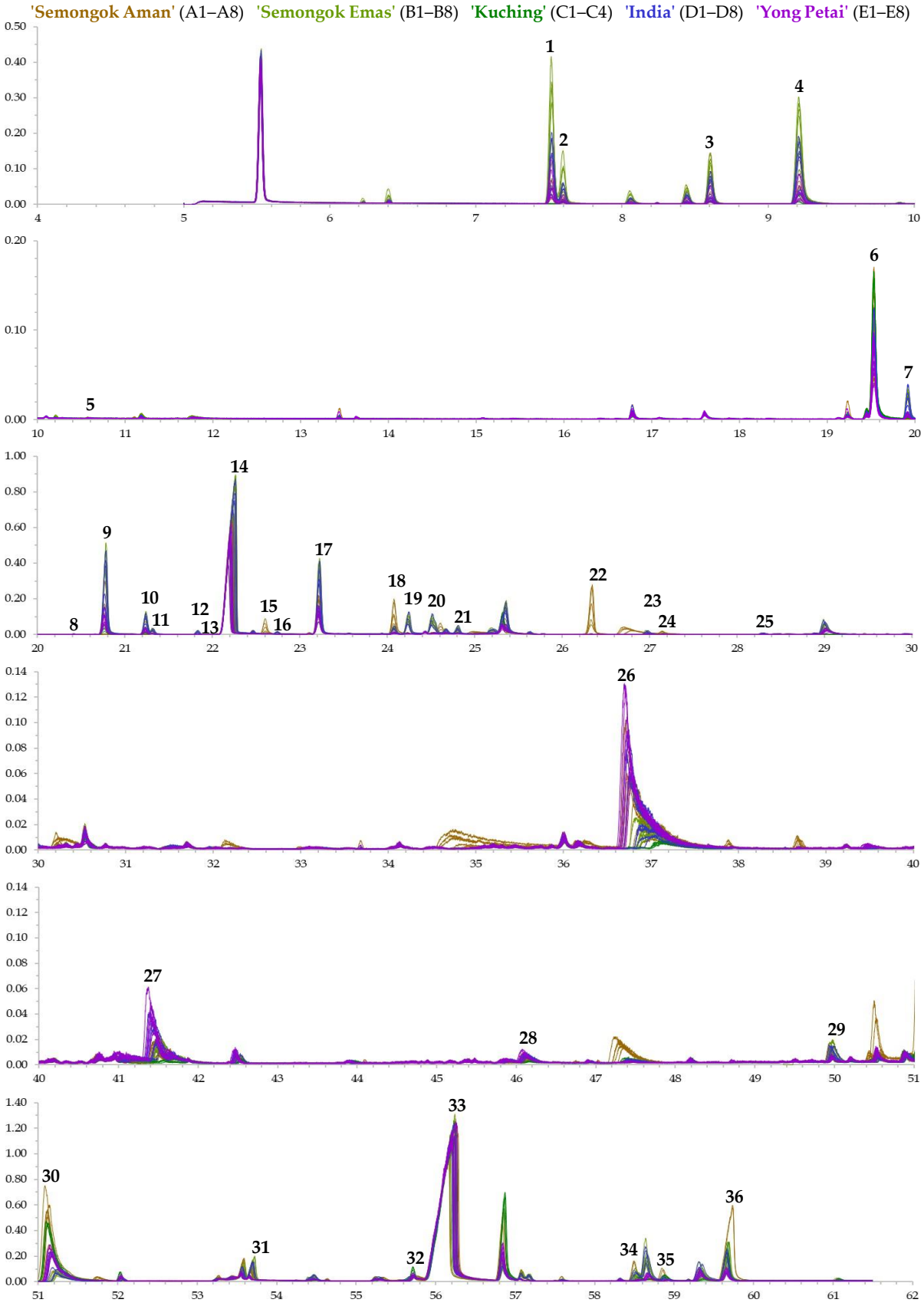

Figure S15. Overlaid and magnified BPCs of *n*-hexane fruit extracts of *Piper nigrum* cultivars. The metabolites of the numbered peaks are listed in Table S2

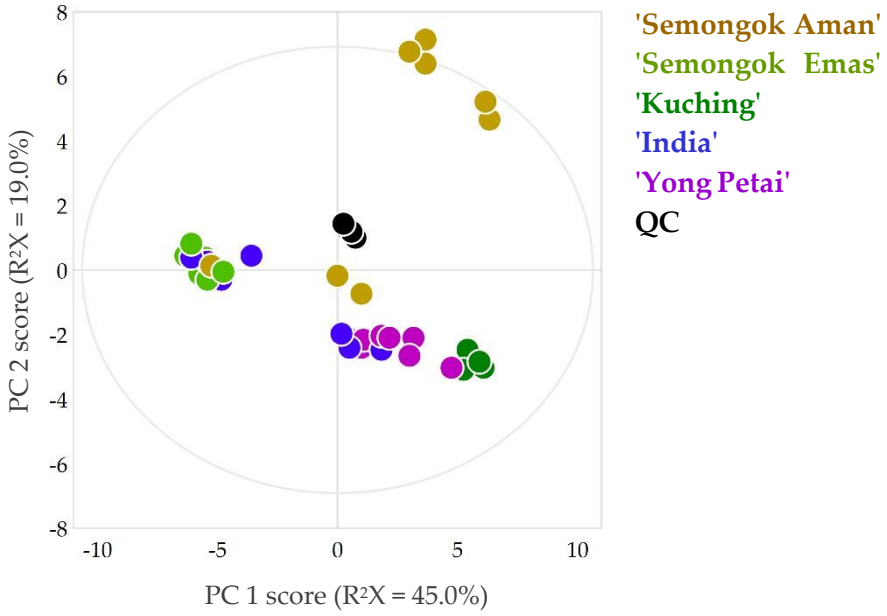

Figure S16. PCA scores scatter plot of preprocessed (matricised, logarithm with base 10 (log10)-transformed, and mean-centred) GC-MS BPCs of *n*-hexane fruit extracts of *Piper nigrum* cultivars (Q^2X [cum. PC 2] = 59.0%). The clustering of all QC samples (black circles) near the centre of the plot indicates that the GC-MS system was stable throughout the run sequence and resulted in a data set of acceptable quality. Dimension of the data matrix = 42 × 370

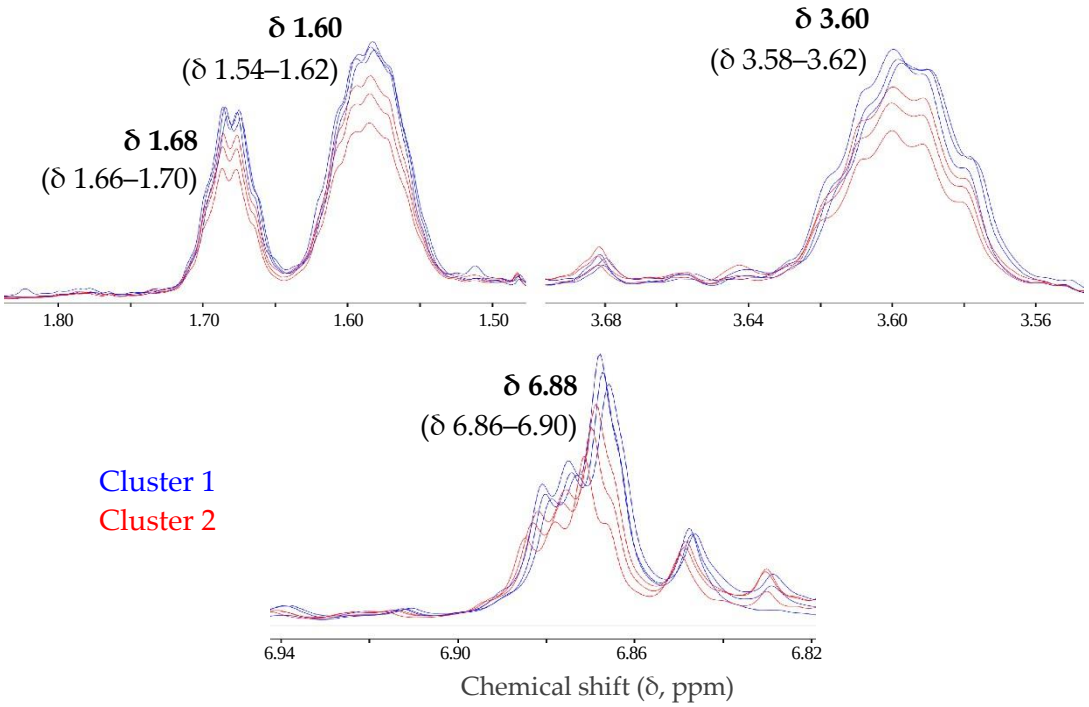

Figure S17. ^{1}H-NMR signals corresponding to the four high-magnitude variables circled in Fig. 3c that discriminate the two clusters of *Piper nigrum* cultivars. Range of L^2 norm of the four discriminating variables = 0.28–0.55, whereas the range of L^2 norm of the other well- modelled variables = 0.06–0.16

Table S1. MZmine 2.53 parameter settings for generation of the FBMN feature list

Parameter	Setting	Parameter	Setting
Mass detection (MS1)		Peak finder (multithreaded)	
Scans	MS level: 1, polarity: +, spectrum type: centroided	Intensity tolerance	10.0%
Mass detector	Centroid, noise level: 5.0×10^4	*m/z* tolerance	0.001 *m/z* or 3.0 ppm
Mass detection (MS2)		RT tolerance	0.1 absolute (min)
Scans	MS level: 2, polarity: +, spectrum type: centroided	Feature list rows filter	
Mass detector	Centroid, noise level: 5.0×10^4	Minimum peaks in a row	1
ADAP chromatogram builder		Peak duration range	0.00–0.30
Scans	MS level: 1, polarity: +, spectrum type: centroided	Keep or remove rows	Keep rows that match all criteria
Min group size in # of scans	5	Keep only peaks with MS2 scan (GNPS)	True
Min height	3.0×10^3	Reset the peak number ID	True
Group intensity threshold	1.0×10^5	Duplicate peak filter	
Min highest intensity	1.0×10^5	Filter mode	Old average
m/z tolerance	0.001 *m/z* or 5.0 ppm	*m/z* tolerance	0.001 *m/z* or 3.0 ppm
Chromatogram deconvolution			
Algorithm	Wavelets (ADAP), S/N threshold: 30, S/N estimator: intensity window SN, min feature height: 10,000,000, coefficient/area threshold: 150, peak duration range (min): 0.05–0.50; RT wavelet range: 0.00–0.05	RT tolerance	0.1 absolute (min)
m/z center calculation	Median	Export for/submit to GNPS	
Isotopic peaks grouper		Filter rows	Only with MS2
m/z tolerance	0.001 *m/z* or 3.0 ppm		
RT tolerance	0.09 absolute (min)		
Monotonic shape	True		
Maximum charge	3		
Representative isotope	Most intense		
Join aligner			
m/z tolerance	0.001 *m/z* or 3.0 ppm		
Weight for *m/z*	0.9		
RT tolerance	0.1 absolute (min)		
Weight for RT	0.1		
Require same charge state	True		

Table S2. Metabolites of *Piper nigrum* fruit identified in GC-MS metabolomics

No.	RT (min)	LRI	Metabolite	Reference
1	7.52	973	Sabinene	Babushok *et al.* (2011)
2	7.60	975	β-Pinene	Babushok *et al.* (2011)
3	8.60	1010	3-Carene	Babushok *et al.* (2011)
4	9.21	1029	D-Limonene	Babushok *et al.* (2011)
5	10.58	1071	(*Z*)-Sabinene hydrate	Babushok *et al.* (2011)
6	19.53	1338	δ-Elemene	Babushok *et al.* (2011)
7	19.92	1350	α-Cubebene	Babushok *et al.* (2011)
8	20.40	1365	Cyclosativene	Babushok *et al.* (2011)
9	20.77	1376	α-Copaene	Babushok *et al.* (2011)
10	21.23	1391	β-Cubebene	Babushok *et al.* (2011)
11	21.31	1393	β-Elemene	Babushok *et al.* (2011)
12	21.83	1410	α-Gurjunene	Babushok *et al.* (2011)
13	21.95	1414	α-Cedrene	Babushok *et al.* (2011)
14	22.21	1422	(*E*)-β-Caryophyllene	Babushok *et al.* (2011)
15	22.60	1435	γ-Elemene	Babushok *et al.* (2011)
16	22.74	1439	α-Guaiene	Babushok *et al.* (2011)
17	23.21	1454	α-Humulene	Babushok *et al.* (2011)
18	24.10	1482	Germacrene D	Babushok *et al.* (2011)
19	24.23	1487	β-Selinene	Babushok *et al.* (2011)
20	24.51	1496	α-Selinene	Babushok *et al.* (2011)
21	24.80	1506	α-Bulnesene	Babushok *et al.* (2011)
22	26.35	1558	Germacrene B	Babushok *et al.* (2011)
23	26.97	1580	Nerolidol	Miyazaki *et al.* (2011)
24	27.15	1586	Caryophyllene oxide	Adams (2017)
25	28.32	1628	Germacrene D-4-ol	Andriamaharavo (2014)
26	36.79	1945	Pellitorine	Andriamaharavo (2014)
27	41.40	2154	Neopellitorine B	Andriamaharavo (2014)
28	46.07	2376	(2*E*,4*E*)-1-(Piperidin-1-yl)dodeca-2,4-dien-1-one	Andriamaharavo (2014)
29	49.96	2576	(2*E*,4*E*)-*N*-Isobutylhexadeca-2,4-dienamide	Andriamaharavo (2014)
30	51.20	2652	Piperanine	Andriamaharavo (2014)
31	53.65	2781	Pipericine	Andriamaharavo (2014)
32	55.62	2896	Trichostachine	Andriamaharavo (2014)
33	56.20	2931	Piperine	Andriamaharavo (2014)
34	58.43	3068	Retrofractamide A	Andriamaharavo (2014)
35	58.88	3096	Tricholein	Andriamaharavo (2014)
36	59.78	3155	Piperolein B	Andriamaharavo (2014)

Table S3. ^{1}H-NMR chemical shifts of piperine

H	δ_H	
	Present research (buffered 50% CD_3OD, 500 MHz)	Traxler *et al.* (2020) (CD_3OD, 600 MHz)
4		6.91 (ddd)
5	6.86–6.90	6.84 (d)
5"		6.80 (d)
2', 6'	3.58–3.62	3.63 (t)
3', 5'	1.54–1.62	1.59 (m)
4'	1.66–1.70	1.71 (m)

REFERENCES (FOR SUPPLEMENTARY MATERIALS)

Adams, R.P. (2017). *Identification of essential oil components by gas chromatography/mass spectrometry*. Fourth Edition. DuPage County: Allured Business Media.

Andriamaharavo, N.R. (2014). Retention Data. NIST Mass Spectrometry Data Center. https://webbook.nist.gov/cgi/cbook.cgi?Source=2014AND%2319410M&Mask=2000

Babushok, V.I., Linstrom, P.J. & Zenkevich, I.G. (2011). Retention indices for frequently reported compounds of plant essential oils. *Journal of Physical and Chemical Reference Data*, 40(4): 043101. DOI: 10.1063/1.3653552

Miyazaki, T., Plotto, A., Goodner, K. & Gmitter, F.G. (2011). Distribution of aroma volatile compounds in tangerine hybrids and proposed inheritance. *Journal of the Science of Food and Agriculture*, 91(3): 449–460. DOI: 10.1002/jsfa.4205

Traxler, F., Schinnerl, J. & Brecker, L. (2020). Spectroscopic studies on the molecular interactions of curcumin and piperine. *Monatshefte Fur Chemie*, 151(3): 325–330. DOI: 10.1007/s00706-020-02563-z